ELSEVIER

Radiance Calibration of DMSP-OLS Low-Light Imaging Data of Human Settlements

Christopher D. Elvidge,[*] *Kimberly E. Baugh,*[†] John B. Dietz,[‡] Theodore Bland,[§] *Paul C. Sutton,*[‖] *and Herbert W. Kroehl*[¶]

Nocturnal lighting is a primary method for enabling human activity. Outdoor lighting is used extensively worldwide in residential, commercial, industrial, public facilities, and roadways. A radiance calibrated nighttime lights image of the United States has been assembled from Defense Meteorological Satellite Program (DMSP) Operational Linescan System (OLS). The satellite observation of the location and intensity of nocturnal lighting provide a unique view of humanities presence and can be used as a spatial indicator for other variables that are more difficult to observe at a global scale. Examples include the modeling of population density and energy related greenhouse gas emissions. Published by Elsevier Science Inc.

INTRODUCTION

Much of global change research is dedicated to discerning and documenting the impacts of human activities on natural systems. Human population numbers have expanded from ~750 million in the mid-1700s, will reach 6 billion in 1999, and could double in the next 49 years if current growth continues (Haub and Cornelius, 1998). Human activities which are known to be cumulatively altering the global environment include greenhouse gas emissions from fossil fuel consumption, air and water pollution, and land cover/land use change.

Far from being evenly distributed across the land surface, to a great extent human activities with environmental consequences are concentrated in or near human population centers. One approach to modeling the spatial distribution of human activities is to use population density as an indicator for the phenomenon of interest (e.g., the percent coverage of impermeable surfaces). There are two primary disadvantages to using population density as an indicator for human activities with environmental consequences. At a global level, population density is not well characterized. Currently available global population density grids cover approximately 60 sq km per data cell (Tobler et al., 1995), far too coarse for many environmental applications. In areas where high spatial resolution population density data sets are available, the environmental applicability of the data suffer due to the fact that population density is defined as a residential parameter. As a result transportation corridors, public, commercial, and industrial zones have very low population density. In many cases these areas have much higher densities of people present 8–12 h/day than the associated residential zones. Thus the use of population density as an indicator for percent of land area covered by impermeable surface (roads, roofs, parking lots) would result in a substantial skewing of the results towards residential areas.

Having a capability for direct global observation of a widespread and distinctly human activity that varies in intensity could substantially improve understanding of the magnitude of humanities presence and modeling human impacts on the environment. Available satellites sensors with global data acquisition capabilities have all focused on the observation of natural systems as their design criteria. If global observation of human activity

[*] NOAA National Geophysical Data Center, Boulder
[†] Cooperative Institute for Research in Environmental Sciences, University of Colorado, Boulder
[‡] Cooperative Institute for Research on Atmosphere, Colorado State University, Fort Collins
[§] Electronic Sensors and Systems Division, Northrop Grumman Corporation, Baltimore
[‖] Department of Geography, University of California, Santa Barbara
[¶] Solar-Terrestrial Physics Division, NOAA National Geophysical Data Center, Boulder

Address correspondence to C. D. Elvidge, NOAA National Geophysical Data Center, 325 Broadway, Boulder, CO 80303. E-mail: cde@ngdc.noaa.gov

Received 9 May 1998; revised 2 October 1998.

REMOTE SENS. ENVIRON. 68:77–88 (1999)
Published by Elsevier Science Inc.
655 Avenue of the Americas, New York, NY 10010

0034-4257/99/$–see front matter
PII S0034-4257(98)00098-4

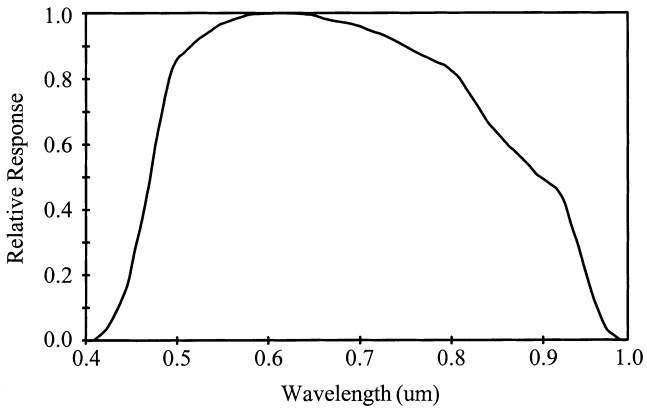

Figure 1. Bandpass for the visible band for the OLS instrument aboard DMSP F-12.

was set as a design criteria, what wavelength(s) would be investigated? Radio frequencies emitted by power lines, electrical devices, and cellular telephones might be a good starting point! As an alternative, we have been investigating the nocturnal observation of artificial lighting as a measure or indicator of human activity using data collected by the U.S. Air Force Defense Meteorological Satellite Program (DMSP) Operational Linescan System (OLS). This instrument has a low-light imaging capability, which was designed for the observation of clouds illuminated by moonlight. In addition to moonlit clouds, the data can be used to detect light sources present at the Earth's surface.

We have explored the gain control of the OLS and discovered that it is possible to adjust the gain to cover the range of radiances encountered from brightly lit commercial centers in the largest cities down to residential areas in urban, suburban, and many rural settings. The OLS low-light imaging data can be converted to brightness values based on the preflight calibration of the OLS sensor. The objective of this article is to review the low-light imaging features of the OLS, to describe methods used for the assembly of radiance calibrated nighttime lights products of the United States, and to compare this product to several other data types.

BACKGROUND

Since 1970 the DMSP has operated polar orbiting satellite sensors capable of low-light imaging the Earth at night. Using light intensifying photomultiplier tube technology, these sensors were designed to observe clouds illuminated by moonlight using a single broad spectral band (Fig. 1). With sunlight eliminated, it possible to also detect city lights, gas flares, and fires. From 1970 to 1975 DMSP Blocks 5A, B, and C flew equipped with the SAP (*S*ensor *A*erospace Vehicle Electronics *P*ackage). The Operational Linescan System (OLS) first flew on DMSP Block 5D-1 satellite F-1, launched in September 1976. In 1999, DMSP operates three OLS (satellites F-12, F-13, and F-14). Many details of the OLS instrument and the onboard data processing are described by Lieske (1981).

The OLS is an oscillating scan radiometer which generates images with a swath width of ~3000 km. With 14 orbits per day, each OLS is capable of generating global daytime and nighttime coverages of the Earth every 24 h. The full resolution data, having a ground sample distance (GSD) of 0.56 km, is referred to as "fine." Onboard averaging of five by five blocks of fine data produces "smoothed" data with a GSD of 2.7 km. The "visible" bandpass straddles the visible and near-infrared (VNIR) portion of the spectrum (Fig. 1). The thermal infrared channel has a bandpass covering 10–13 μm. The visible band has 6-bit quantization, producing digital number (digital number) values ranging from 0 to 63. The thermal infrared band has 8-bit quantization (digital number range from 0 to 255). A constellation of two satellites provides for global coverage four times a day: dawn, day, dusk, and night. Satellite attitude is stabilized using four gyroscopes (three-axis stabilization), a star mapper, Earth limb sensor, and a solar detector.

The potential use of nighttime OLS data for the observation of city lights and other VNIR emission sources was first noted in the 1970s by Croft (1973; 1978; 1979). Welch (1980) and Foster (1983) speculated that OLS data could be used to map the distribution human settlements and inventory the spatial distribution of human activities, such as energy consumption. Sullivan (1989) produced a 10 km resolution global image of OLS observed VNIR emission sources using film data. The global map published by Sullivan (1989) was derived from single dates of OLS imagery, selected based on the presence of large number cloud-free VNIR emission sources and mosaicked into a global product. As a result, many of the features presented in areas such as Africa are ephemeral VNIR emissions from fires. These early studies with OLS data relied on the analysis of film strips, which limited the scope of the studies.

In 1992 the U.S. Air Force and NOAA established a digital archive for DMSP data at the NOAA National Geophysical Data Center. Subsequently, algorithms have been developed to identify and geolocate VNIR emission sources in nighttime OLS imagery (Elvidge et al., 1997a). NGDC has produced a global inventory of fires, gas flares, fishing lightboats, and human settlements using DMSP-OLS observations acquired between 1 October 1994 through 31 March 1995. The thermal infrared band OLS data are used to identify clouds, and the number of times lights are detected in cloud-free areas are tallied. By dividing this tally by the total number of cloud-free observation, it is possible to normalize the frequency of the lights for differences in the number of usable observations. The percent frequency values are then thresholded to eliminate ephemeral events like noise,

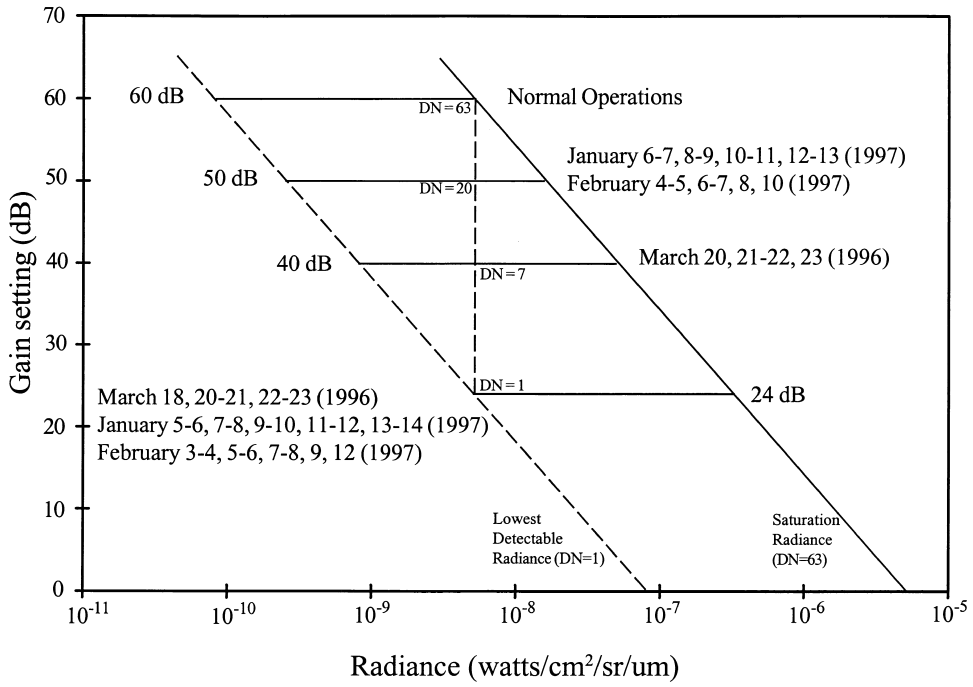

Figure 2. Relationship between the F-12 OLS visible band gain when operated in PMT mode, digital numbers, and observed radiances derived from the preflight sensor calibration.

lightning, and fires. Our experience indicates that most ephemeral events can be eliminated by deleting detections which occurred in less than 6–10% of the cloud-free observations for a time series spanning a 6-month time period. The finished stable lights data record the percent frequency with which lights were observed within the set of cloud-free observations.

Stable lights for the 1994–1995 time period have been produced for most of the Americas, Europe, Asia, and northern Africa (Elvidge et al., 1997b). Sutton et al. (1997) examined the potential use of the stable lights data to spatially apportion population. Imhoff et al. (1997a,b) used the stable lights to estimate the extent of land areas withdrawn from agricultural production. Gallo et al. (1995) used nighttime lights to assess urban heat island impacts on meteorological records. Elvidge et al. (1997b,c) found that the area lit (km^2) from the stable lights of individual counties to be highly correlated to Gross Domestic Product.

The stable lights product indicates the percent frequency with which lights were detected within the set of cloud-free observations, with no indication of the brightness of the lights. The stable lights products were assembled utilizing data acquired under low lunar illumination conditions, making it is possible to exclude moonlit clouds and reservoirs from the analysis. The high gain settings (or amplification) used during the dark half of the month make it possible to detect faint sources of VNIR emission, but result in saturated data for many urban areas. This prevented implementation of a radiance calibration in our earliest nighttime lights products.

OLS LOW-LIGHT IMAGING GAIN CONTROL

An optical instrument's gain can be thought of as the amplification of the incoming signal, from the front end of the telescope to the output of the digital number data stream. The full system contains both gains and losses; however, the overall system amplifies the original signal. The OLS has analog preamplifiers and postamplifier with fixed gains as well as VDGA (Variable Digital Gain Amplifier) gain. The gain of the photomultiplier tube (PMT) also contributes to the overall system gain for night scenes. Primary control of the low-light imaging gain is achieved through ground command of the VDGA, which has values from 0 to 63 decibels (dB is the log of the amplification).

Prior to launch, the OLS is calibrated under conditions which simulate the space environment. During the calibration the OLS views light sources having known irradiance, and digital numbers are recorded over the full range of VDGA. The calibration data equate telescope input illuminance to digital numbers at specific VDGA gain settings.

Figure 2 shows the relationship between OLS VDGA gain settings and the observed range of radiances, based on the preflight sensor calibration. This calibration data makes it possible to relate OLS digital numbers back to the laboratory observed radiances known in terms of W/cm^2/sr/μm. The solid diagonal line indicates the saturation radiance (digital number=63). Observed pixels with radiances greater than this radiance yield digital number values of 63. The dashed diagonal line indicates the radiance for a digital number of 1, the lowest

detectable radiance. At a VDGA gain setting of 63, the full system gain, including the fixed gain amplifiers, is 136 dB. This is a light intensification of $10^{13.6}$ times the original input signal, permitting measurement of radiances down to 10^{-10} W/cm ^{2}/sr/μm. This is approximately 6 orders of magnitude lower than the OLS daytime visible band or the VNIR bands of other sensors, such as the NOAA AVHRR or the Landsat Thematic Mapper.

The primary objective of the on-orbit OLS gain control is the generation of consistent imagery of clouds at all scan angles for visual interpretation by Air Force meteorologists. In normal operations the VDGA is modified to track scene illumination predicted from lunar phase and elevation. The resulting base gains are modified every 0.4 ms by an onboard along scan gain control (ASGC) algorithm. In addition, a BRDF (bidirectional reflectance distribution function) algorithm further adjusts the gain in the scan segment where the illumination angle equals the observation angle.

The lowest gain settings occur under full moon conditions, producing imagery which looks strikingly similar to daytime visible band data. Gain settings gradually rise as lunar illumination declines, reaching levels at or near 60 dB (Fig. 2) between the last quarter and first quarter lunar phases. During the darkest 10 nights of each lunar cycle, illumination is too low to detect clouds in the OLS visible band data, even with high gain settings. Under these conditions the effects of the along scan gain and BRDF algorithms are minimized, and the gain rises to its maximum monthly level.

DATA ACQUISITION

In early 1996, NGDC requested and received permission from the DMSP program office to acquire OLS data at reduced gain settings, with onboard ASGC (along scan gain control) and BDRF functions turned off. The "low-gain" data acquisition was requested for an 8-night period, corresponding to the darkest nights in March 1996, with a start date of 16 March. In order to avoid interference with ongoing observations of the leading edge of the aurora at high northern latitudes, the NGDC request was for the acquisition of reduced gain nighttime visible band data for the −55° to 55° latitude range. The northern limit of the usable data was reduced to latitudes less than 45° due to the presence of solar glare (see Fig. 3).

Because the OLS gain had never been operated with the objective of observing the brightness patterns of light sources present at the Earth's surface, there was no *a priori* information available on what gain setting would be required to avoid saturation on major urban centers. To address this question, OLS data was acquired at a series of VDGA gain settings, by switching the gain in a steplike fashion for the first 24 h of the 8-day period. An example of this data is shown in Figure 3.

On 17 March the step-gain OLS data values of major urban centers were examined to determine extent of saturation. This examination lead to the selection of a VDGA gain setting of 26 dB for use in the second 24 h. It was found that this gain setting continued to produce saturated data in the bright centers of major cities and the gain level was reduced to 24 dB for the third 24-h period. Very few urban centers continued to have saturated pixels in the data acquired at 24 dB. For example, a set of three saturated OLS pixels were found in the center of Las Vegas, Nevada. However, at this low gain setting, only the bright cores of urban centers were detected. To detect the larger number of the smaller and dimmer sites, it was decided to acquire data with gain settings of 40 dB on the fourth 24-h period and to then alternate between 24 dB and 40 dB every 24 h (Fig. 2).

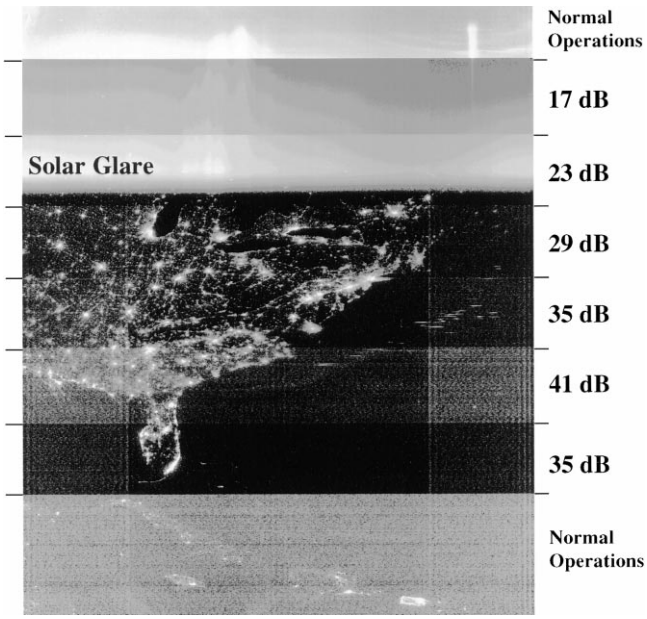

Figure 3. F-12 OLS visible band data acquired with a range of gain settings on 16 March 1996.

Initial examination of the 1996 low-gain revealed that it is possible to observe brightness variations within urban centers. A global radiance calibrated product could not yet be assembled due the presence of solar glare at latitudes greater than 45° and the relatively small number of orbits available at each gain setting. It was also concluded that a gain setting higher than 40 dB would be required to detect the large numbers of small towns detected in the 1994–1995 stable lights products. As a result, NGDC requested and received additional low-gain data acquisitions for 5–14 January and 3–12 February 1997 from −65° to 75° latitude, using alternating gain settings of 24 dB and 50 dB (Fig. 2). These correspond to the 10 darkest nights of January and February 1997.

DATA PROCESSING

As a first step in the processing, sections (suborbits) of usable nighttime lights data were extracted from the

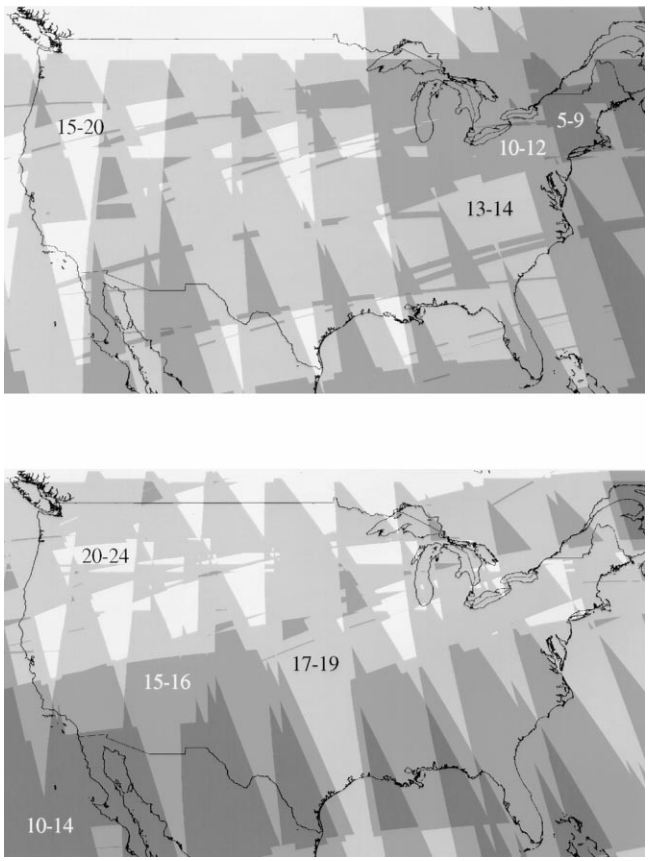

Figure 4. Total number of data coverages for observations made at gains greater than 30 dB (top) and for observations made at gains less than 30 dB (bottom).

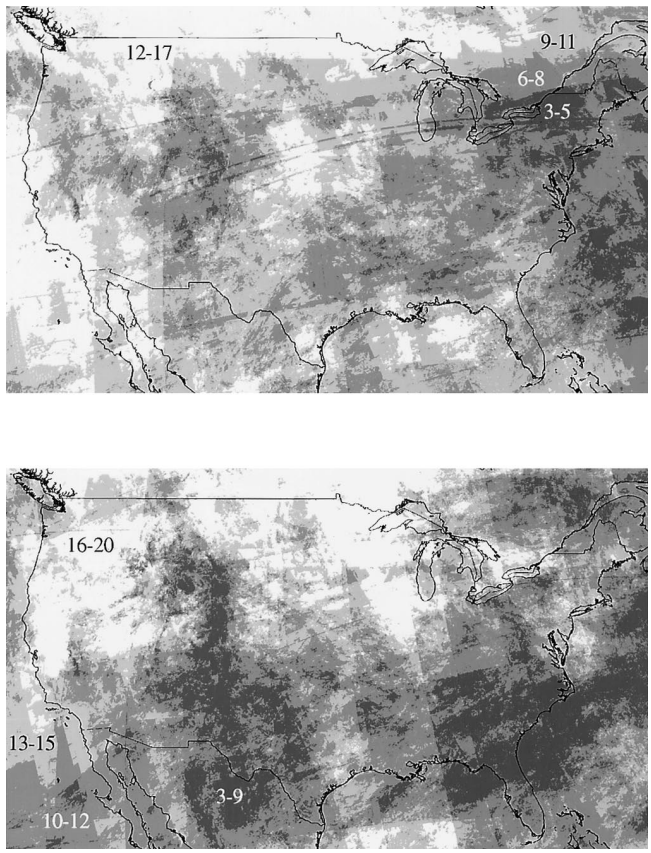

Figure 5. Total number of cloud-free data coverages for observations made at gains greater than 30 dB (top) and observations made at gains less than 30 dB (bottom).

original full orbit files. The data processing then involved the following primary steps: 1) establishment of a reference grid; 2) identification and geolocation of lights, clouds, and coverage areas; 3) establishing a digital number to radiance scale for the final product; 4) cloud-free compositing within two overlapping gain ranges (high and low); 5) threshold to eliminate isolated detections; and 6) combine the calibrated images from the two gain ranges by averaging based on the number of detections.

1. Reference Grid: Development of a spatially coherent temporal image composite requires the use of a reference grid with finer spatial resolution than the input imagery. We have used the 1 km equal area Interrupted Goode Homolosine Projection (Goode, 1925; Steinwand, 1993) developed for the NASA-USGS Global 1 km AVHRR project (Eidenshink and Faundeen, 1995). The IGHP is optimized to provide a uniform grid cell size at all latitudes and contiguous land masses (except Antarctica). These are favorable characteristics for the production of global land datasets from raster imagery (Steinwand, 1993).

2. Identification and Geolocation of Lights, Clouds, and Coverages: Data gaps within suborbits are filled with digital number values of zero. The outline of each block of valid data was identified using an automatic program which draws a polygon at the edges of the scan and along the edges of data gaps. These polygons are ultimately used to track the total number of cloud-free observations within the reference grid.

In our previous nighttime lights products, lights were detected using an automatic algorithm that established a local threshold based on background brightness levels (Elvidge et al., 1997a). This methodology was developed to reduce human involvement in the identification of the lights, to contend with the high noise levels typically encountered (see bottom section of imagery in Fig. 3), and to permit processing at all lunar illumination conditions.

The local thresholding algorithm operates very quickly and identifies lights from major cities and towns (points of light) under a wide range of conditions. However, the algorithm does not generally detect "diffuse lighting," which is dim and scattered across the landscape. These areas can be observed in OLS data in locations like the northeastern United States and surrounding major metropolitan areas.

We found that noise was greatly reduced in the data that were acquired for our study. In an attempt to identify areas of diffuse lighting as well as lights in focused centers such as cities and towns, we developed a soft-

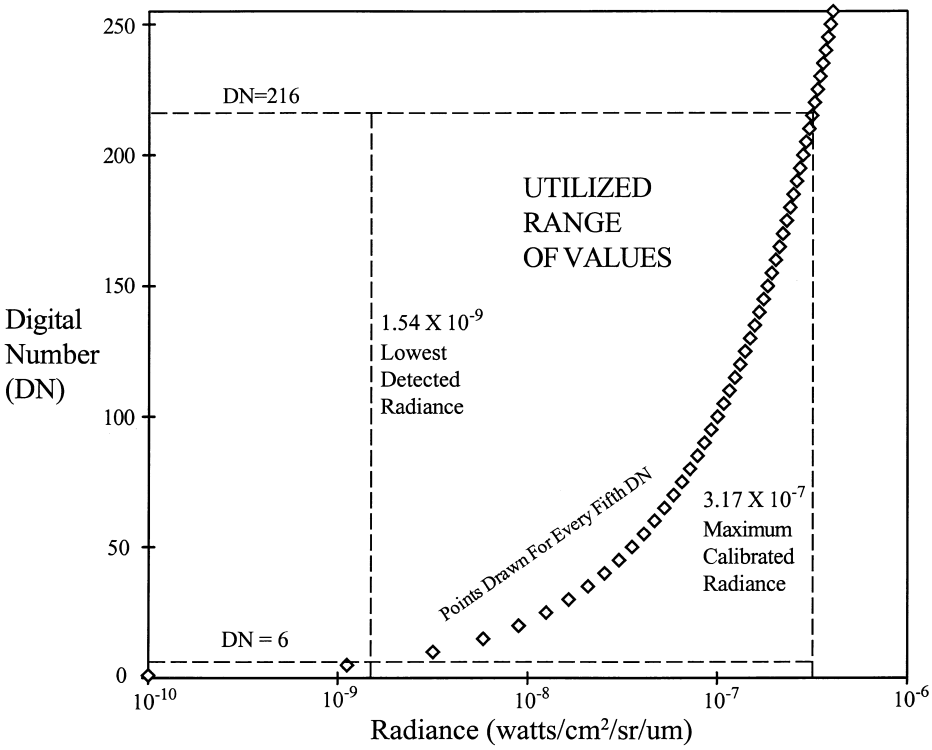

Figure 6. Digital number versus radiance diagram for the composited output product.

ware tool that an image analyst can use to select a threshold a single digital number above the noise level encountered in a suborbit. An image analyst then reviewed each suborbit, selecting thresholds, which were used to extract pixels with detectable levels of VNIR emission. The analyst also identified defective scan lines and scan lines with lightning. In addition, the analyst created image masks for image areas which contained excessive noise or phenomena such as solar glare. Data within the marked scan lines of under the image masks were eliminated from the compositing procedure described below.

Because of the low level of lunar illumination present in the orbital segment, it was not possible to use the visible band to identify clouds. The cloud identification was based entirely on thresholds set on the thermal infrared band. Clouds are generally colder than the Earth's surface. However, the separation of cloud pixels from Earth surface pixels using thermal infrared thresholding is complicated by seasonal, latitudinal, and altitudinal variations in the background Earth surface temperature. The separation of clouds from Earth surface pixels is relatively easy at low latitudes, where there is generally a large temperature difference between pixels of cloud tops and pixels containing land or ocean. Because of the strong latitudinal effects on the thermal infrared threshold for cloud screening in our data, we segment each suborbit into 200-pixel-wide latitudinal bands and visually select a thermal infrared threshold for identification of the cloud pixels.

Figure 7. Radiance calibrated OLS image composites of Minneapolis, Minnesota for two overlapping gain ranges, indicating the use of compositing to overcome the dynamic range limitations of the OLS sensor.

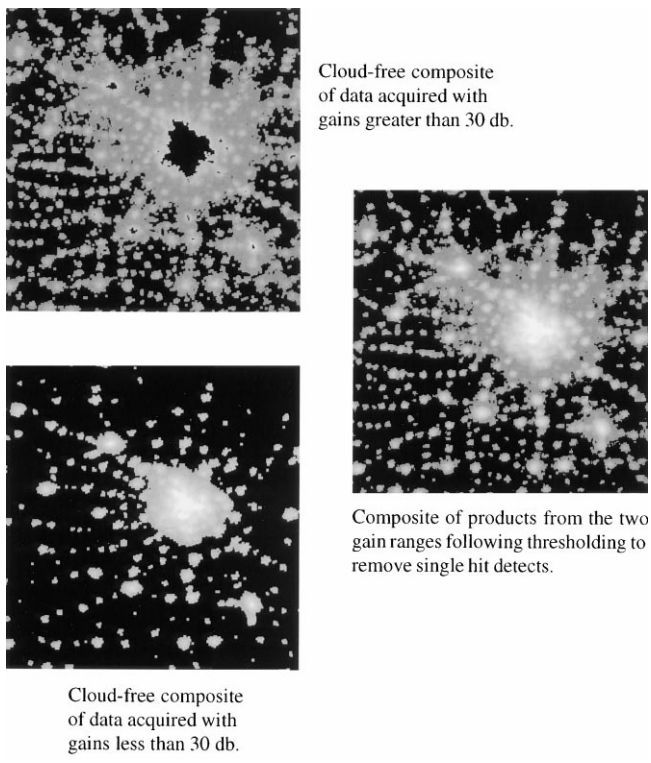

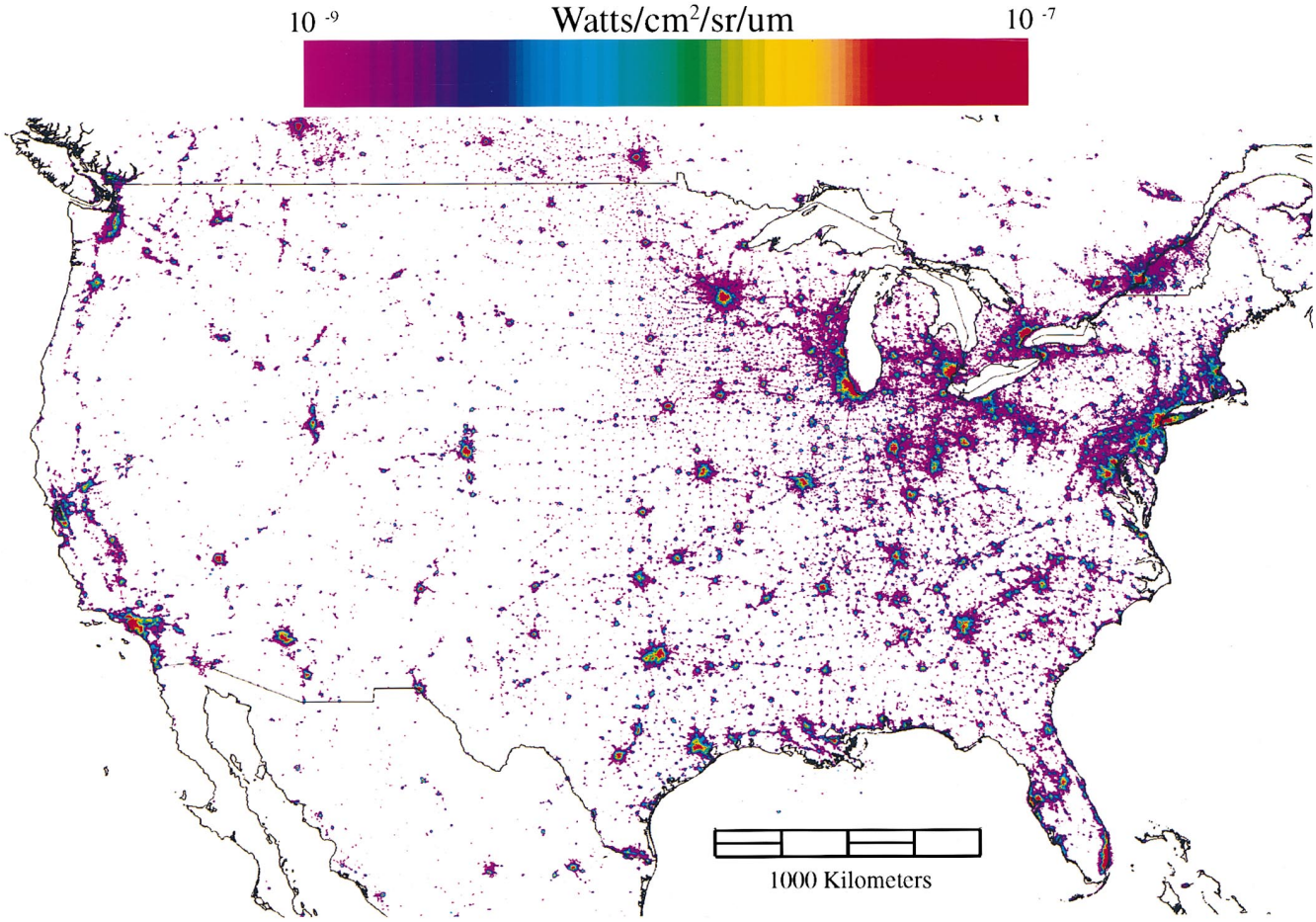

Figure 8. Radiance calibrated nighttime lights of the United States.

Lights, clouds, and the coverage polygons were then geolocated. Our geolocation algorithm operates in the forward mode, projecting the center point of each pixel onto the Earth's surface. The geolocation algorithm estimates the latitude and longitude of pixel centers based on the geodetic subtrack of the satellite orbit, satellite altitude, OLS scan angle equations, an Earth sea level model, and digital terrain data. The geodetic subtrack of each orbit is modeled using daily radar bevel vector sightings of the satellite (provided by Naval Space Command) as input into an Air Force orbital mechanics model that calculates the satellite position every 0.4208 s. The satellite heading is estimated by computing the tangent to the orbital subtrack. We have used an oblate ellipsoid model of sea level and have used 30 arc second digital terrain data provided by the U.S. Geological Survey, EROS Data Center.

3. Digital Number to Radiance Scale: The thresholds for the light detection established the range of radiances which would be encompassed in the output product. The lowest radiances, detected in data acquired with a gain of 50 dB, was 1.54×10^{-9} W/cm^2/sr/μm. The maximum calibrated radiance observed was 3.17×10^{-7} W/cm^2/sr/μm. In establishing a digital number to radiance conversion scale, we had two criteria: 1) The digital number data in byte format (0–255), and 2) the scale should exceed the range of current data to accommodate later extensions made at lower or higher OLS gain settings. We developed a logarithmic scaling using the function: Radiance=(digital number)$^{3/2}\times10^{-10}$ W/cm^2/sr/μm (Fig. 6).

4. Compositing within High and Low Gain Ranges: Suborbits were divided into two, roughly equal data volume groups: A) data acquired at gains less than 30 dB and B) data acquired at gains greater than 30 dB.

To determine the total number of "cloud-free" observations, the data coverage polygons and cloud detections are tallied within the reference grid. Subtraction of these two images yields the number of cloud-free observations in the time series. This was performed to both the less than and greater than 30 dB data sets (Figs. 4 and 5) to ensure that each land surface area had multiple valid observations. Inspection of the images in Figure 5 revealed that land areas had at least three cloud-free observations in both gain ranges.

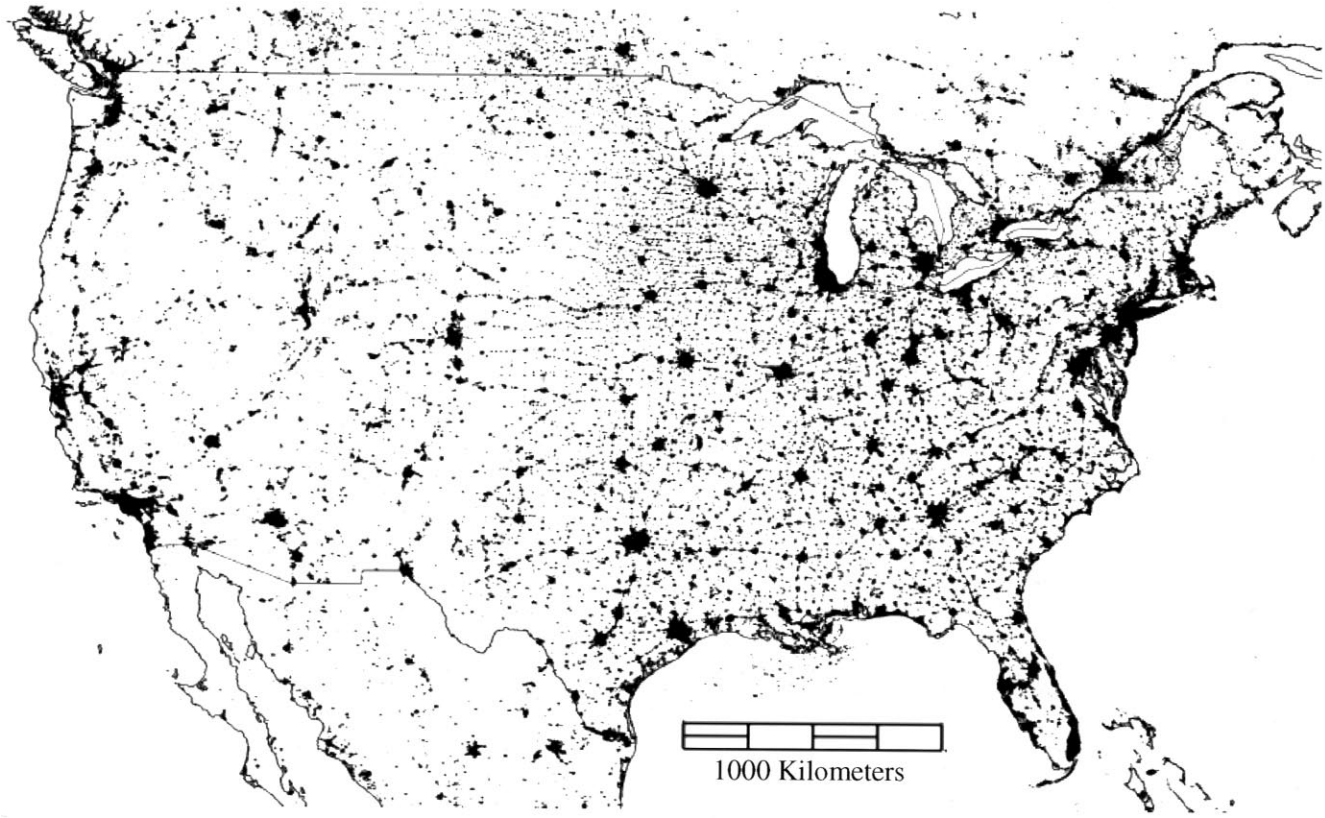

Figure 9. Stable lights of the United States derived from a 1994–1995 DMSP-OLS time series (Elvidge et al., 1997a).

The second step in the preliminary compositing stage is to tally the number of light detections and to produce an average radiance for each reference grid pixel with light detection.

5. Thresholding: The high and low gain composite images were filtered to eliminate detections which occurred only once. This step removes noise and many ephemeral events such as fires or lightning.

6. Combining High and Low Gain Composites: The high and low gain cloud-free composites are averaged. The radiance calibrated digital number average from each image is weighted by the total number of detections. Images demonstrating this final step in the product generation are shown in Figure 7.

RESULTS AND DISCUSSION

Figure 8 is a color-coded image of the radiance calibrated nighttime lights of the United States from 1996–1997. For comparison, the 1994–1995 stable lights product of the United States (Elvidge et al., 1997a), is shown in Figure 9. As with the 1994–1995 stable lights data, the radiance calibrated product shows the cities and many of the smaller towns of the United States. Two major differences have been identified in the spatial information content of the radiance calibrated lights when compared to the stable lights: 1) The radiance calibrated lights provide spatial detail related to brightness variations within urban centers (Fig. 10) that was not present in the stable lights. 2) The radiance calibrated lights show low levels of "diffuse lighting" (shown as purple on Fig. 8) in densely populated rural environments in the Washington, DC to Boston corridor, western Pennsylvania, Indiana, Michigan, Wisconsin, and surrounding major metropolitan areas like Minneapolis-St. Paul, Minnesota.

The radiance calibrated nighttime lights are substantially different in character than other available geospatial data sources. Figure 10a shows a Landsat MSS scene of the St. Louis, Missouri region in a traditional "false color" rendition. The information content is primarily land cover and geomorphology. Major roads can be observed, but there appears to be substantial spectral overlap between human settlements and other land cover types. Figure 10b shows a color-coded version of population density, processed from 1990 U.S. Census Bureau data by CIESIN (1996). Note that there is substantial detail present in the St. Louis area but that outside of the metropolitan area the data appear to be in large homogeneous blocks. This is due to the fact the reporting units used in the census data are postal ZIP codes, which can be quite large in rural areas. Figure 10c shows the radiance calibrated nighttime lights data for the same

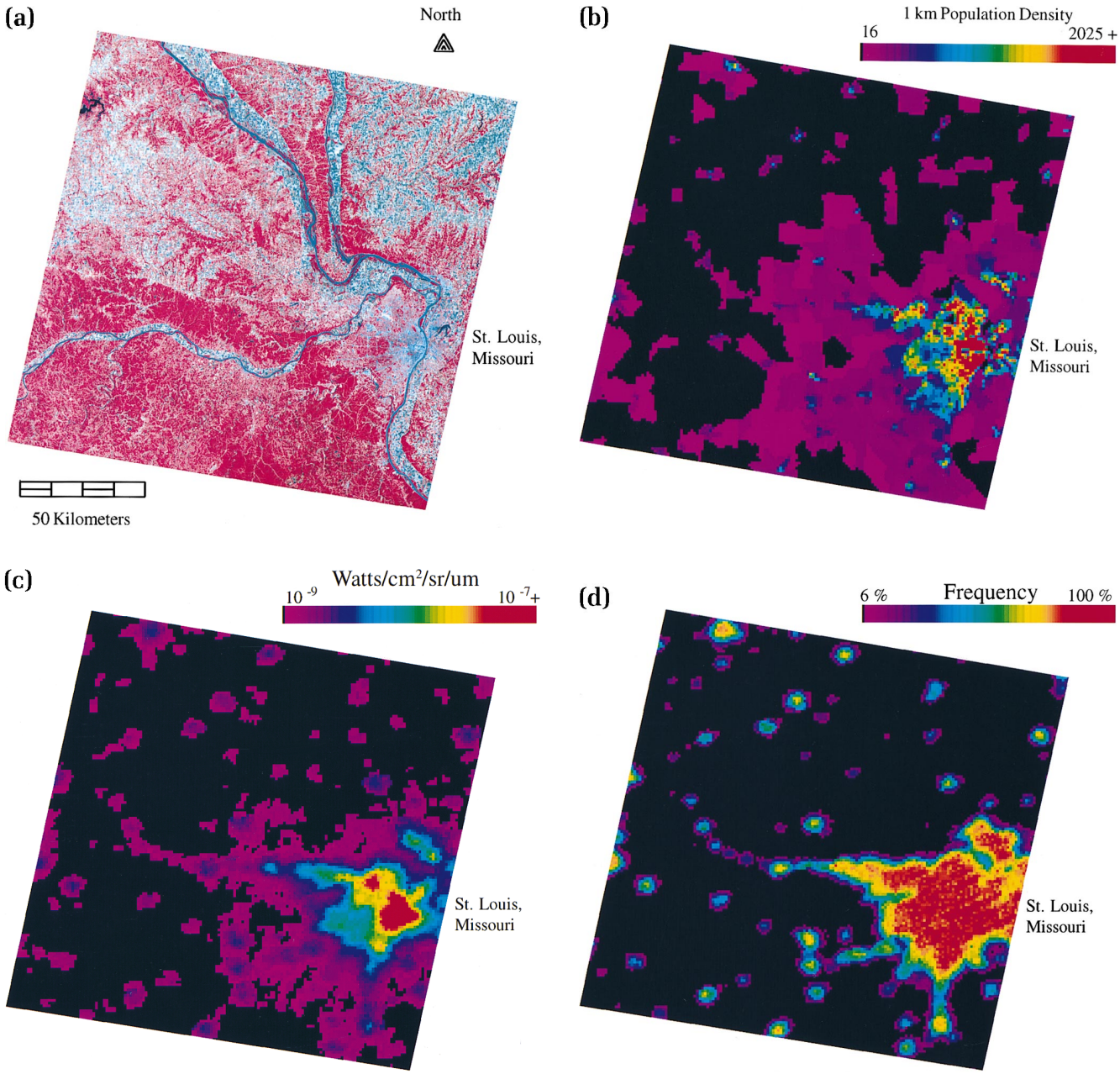

Figure 10. a) Landsat MSS data of the St. Louis, Missouri area, Path 24 Row 33, Bands 4, 2, 1 as red, green, blue, 3 October 1992. b) Population density of the St. Louis, Missouri area in a 1 km grid (CIESIN, 1996). Derived from 1990 U.S. Census Bureau data. c) Radiance calibrated nighttime lights of the St. Louis, Missouri area derived from DMSP-OLS data acquired during March 1996 and January–February 1997. d) Stable lights of the St. Louis, Missouri area derived from a 1994–1995 DMSP-OLS time series.

area. Note that radiance calibrated data is more similar to the population density data than the Landsat data. Close examination of the data in Figures 10b and 10c and more detailed maps indicates that the St. Louis airport and surrounding commercial and industrial zones are quite bright in the radiance calibrated nighttime lights but have low population density. This is one of the busiest areas within the metropolitan region and points out the ability of the OLS data to inventory human activity that is not associated with residences. The 1994–1995 OLS stable lights data are presented in Figure 10d. The units for the stable lights data are percent frequency of detection rather than brightness. The stable light data provide clear indications of the locations of small towns in rural settings, but do not provide the detailed zonation of the radiance calibrated lights within the metropolitan

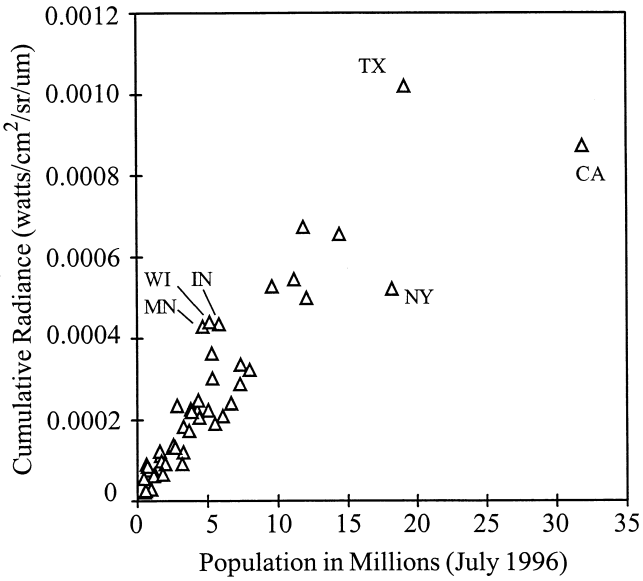

Figure 11. Cumulative radiance from 1996–1997 radiance calibrated DMSP-OLS data versus population in 48 states and the District of Columbia.

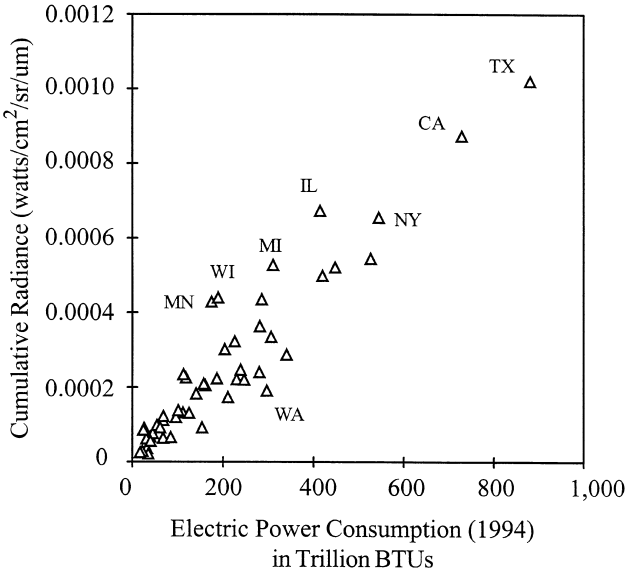

Figure 13. Cumulative radiance from 1996–1997 radiance calibrated DMSP-OLS data versus electric power consumption in 48 states and the District of Columbia.

St. Louis area. In addition, the radiance calibrated lights appear to have better success in detecting the artificial lighting present in sparsely populated rural settings. Detection of lights in these areas begins at about 16 people per sq km.

Major potential applications for the nighttime lights include improved spatial apportionment of human population, energy related greenhouse gas emissions, and environmental factors such as impermeable surfaces. As an initial examination of the potential value of the radiance calibrated lights, we have extracted the cumulative brightness of the 48 states and the District of Columbia and area lit for the same areas from the 1994–1995 stable lights product. These values have been plotted against July 1996 population numbers from the U.S. Census Bureau in Figures 11 and 12. With the exception of California and New York, there is a strongly linear relationship between cumulative radiance and population (Fig. 11). California and New York are anomalously dark relative to their population. We interpret this to be due to the presence of large densely populated areas in New York City and the Los Angeles region. Several states in the upper midwest (Minnesota, Wisconsin, and Indiana) are somewhat brighter than expected based their population numbers.

Figure 12. Area lit from 1994–1995 DMSP-OLS stable lights data (Elvidge et al., 1997a) versus population in 48 states and the District of Columbia.

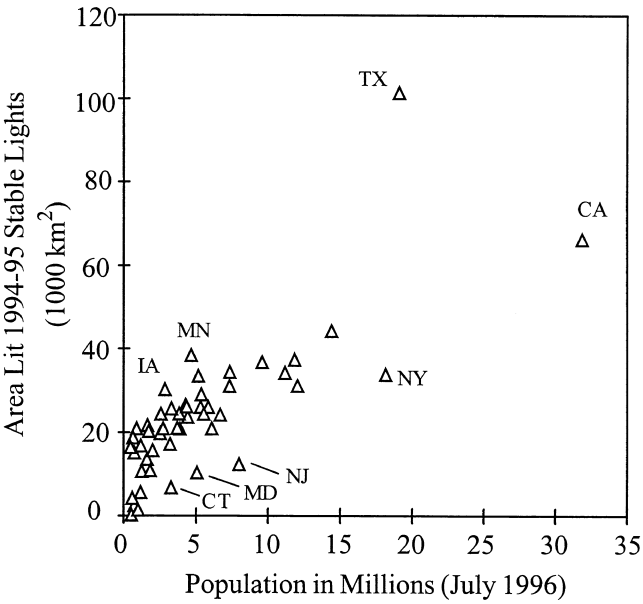

There is considerably more scatter in the relationship between area lit, from the 1994–1995 stable lights, and population numbers (Fig. 12). California, New York, New Jersey, Maryland, and Connecticut all had low area lit values relative to their population numbers.

When cumulative radiance is plotted against 1994 electric power consumption, there is a convergence of points on a well defined axis (Fig. 13). States which are sowewhat brighter than expected are in the upper midwest: Minnesota, Wisconsin, Michigan, and Illinois. The State of Washington is somewhat darker than expected.

CONCLUSION

Nocturnal lighting could be regarded as one of the defining features of concentrated human activity. The spatial

linkage between nocturnal lighting and the locations of concentrated human activity suggests the possibility that observations of the extent or brightness of nocturnal lighting may be used to make spatially explicit estimates population numbers, levels of economic activity, power consumption, or even greenhouse gas emissions.

We have produced a radiance calibrated nighttime lights image of the United States using cloud-free portions of the DMSP-OLS data acquired at reduced gain settings in 1996 and 1997. For the first time since the beginning of DMSP's low light imaging program, it is possible to observe brightness variations within urban centers. Urban brightness variations are normally not observable due to the high gain settings used during normal OLS nighttime operations. The radiance calibrated data are a major advance over the previously produced stable lights product (Elvidge et al., 1997a), which indicated the location of permanent light sources, but had no brightness information.

Producing the radiance calibrated lights involved adjusting the gain on the OLS visible band, the detection and geolocation of VNIR emission sources and clouds for each of the resulting suborbits and a series of compositing steps. Image time series analysis is used to distinguish lights produced by cities, towns, and industrial facilities from sensor noise and ephemeral lights arising from fires and lightning. The time series approach is required in order to ensure that each land area has been covered with sufficient cloud-free observations to determine the presence or absence of VNIR emission sources. Due to the limited dynamic range of the OLS, we used data acquired in overlapping high and low gain settings. Calibration to radiance units has been performed based on the preflight calibration of the OLS.

Initial examination of the radiances values indicates that they are highly correlated with electric power consumption. The lights may prove to be a useful indicator for human activities, such as energy related greenhouse gas emissions. Population is typically tallied based on residence location, rather than workplace. There are locations such as airports, industrial zones, and commercial centers which have low population densities, but high levels of nighttime lighting. Thus it is anticipated that the use of the radiance calibrated lights for the spatially apportion population may, at fine spatial resolution, have imbedded errors. For many applications we anticipate that radiance calibrated nighttime lights would be a better indicator of human activity or human impacts on the environment than population density.

The brightness results indicating that upper midwest states such as Wisconsin and Minnesota are anomalously bright may be due to the presence of highly reflective snow during the January, February, and March data acquisitions. The northern hemisphere winter months are favored for the production of global nighttime lights products due to problems with solar contamination of the OLS visible band data at high latitudes during the April–October time periods. To produce a more uniform global product, it may be necessary to track snow cover as well as cloud cover in the selection of data for compositing. Likewise, it is possible that leaf-on versus leaf-off conditions may effect the observed radiances where deciduous trees are present.

The product demonstrates that it is technically feasible to produce a global map of radiance calibrated nocturnal emissions. The next major advance in our product development will be to add an atmospheric correction, to retrieve estimates of upwelling radiance near the Earth's surface. The DMSP program is expected to continue to operate OLS sensors until at least the year 2010. The NOAA-DoD converged system of meteorological sensors, scheduled for deployment towards the end of that decade, will preserve the low light sensing capability initiated with the OLS. Thus the mapping of VNIR emission sources using nighttime satellite data can be expected to be a continuing source of information for the coming decades.

The authors gratefully acknowledge the Defense Meteorological Satellite Program (DMSP) and the Air Force Weather Agency for their cooperation in the acquisition of the reduced gain OLS data used in this study. This research was supported in part by the NASA EOS Interdiciplinary Science (IDS) Project: Assessing the Impact of Expanding Urban Land Use on Agricultural Productivity Using Remote Sensing Data and Physically-Based Soil Productivity Models.

REFERENCES

CIESIN (Consortium for International Earth Science Information Network) (1996), Population density grid of the USA, Columbia University, New York, NY.

Croft, T. A. (1973), Burning waste gas in oil fields. *Nature* 245:375–376.

Croft, T. A. (1978), Nighttime images of the earth from space. *Sci. Am.* 239:86–98.

Croft, T. A. (1979), The brightness of lights on Earth at night, digitally recorded by DMSP satellite, Stanford Research Institute Final Report, U.S. Geological Survey, Washington, DC.

Eidenshink, J. C. and Faundeen, J. L. (1994), The 1-km AVHRR global land data set: first stages in implementation. *Int. J. Remote Sens.* 15:3443–3462.

Elvidge, C. D., Baugh, K. E., Kihn, E. A., Kroehl, H. W, and Davis, E. R. (1997a), Mapping of city lights using DMSP Operational Linescan System data. *Photogramm. Eng. Remote Sens.* 63:727–734.

Elvidge, C. D., Baugh, K. E., Kihn, E. A., Kroehl, H.W, Davis, E. R., and Davis, C. (1997b), Relation between satellite observed visible–near infrared emissions, population, and energy consumption. *Int. J. Remote Sens.* 18:1373–1379.

Elvidge, C. D., Baugh, K. E., Hobson, V. H., et al. (1997c), Satellite inventory of human settlements using nocturnal radiation emissions: a contribution for the global toolchest. *Global Change Biol.* 3:387–395.

Foster, J. L. (1983), Observations of the Earth using nighttime visible imagery. *Int. J. Remote Sens.* 4:785–791.

Gallo, K. P., Tarpley, J. D., McNab, A. L., and Karl, T. R. (1995), Assessment of urban heat islands: a satellite perspective. *Atmos. Res.* 37:37–43.

Goode, J. P. (1925), The Homolosine projection: a new device for portraying the Earth's surface entire. *Assoc. Am. Geogr. Ann.* 115:119–125.

Haub, C., and Cornelius, D. (1998), *The 1998 World Population Data Sheet*, Population Reference Bureau, Washington, DC.

Imhoff, M. L., Lawrence, W. T., Stutzer, D.C., and Elvidge, C. D. (1997a), A technique for using composite DMSP/OLS "City Lights" Satellite data to accurately map urban areas. *Remote Sens. Environ.* 61:361–370.

Imhoff, M. L., Lawrence, W. T., Elvidge, C., et al. (1997b), Using nighttime DMSP/OLS images of city lights to estimate the impact of urban land use on soil resources in the U.S. *Remote Sens. Environ.* 59:105–117.

Lieske, R. W. (1981), DMSP primary sensor data acquisition. *Proc. Int. Telemetering Conf.* 17:1013–1020.

Steinwand, D. R. (1993), Mapping raster imagery into the interrupted Goode Homolosine Projection. *Int. J. Remote Sens.* 15:3463–3472.

Sullivan, W. T., III (1989), A 10 km resolution image of the entire night-time Earth based on cloud-free satellite photographs in the 400–1100 nm band. *Int. J. Remote Sens.* 10:1–5.

Sutton, P., Roberts, D., Elvidge, C., and Meij, H. (1997), A comparison of nighttime satellite imagery and population density for the continental United States. *Photogramm. Eng. Remote Sens*. 63:1303–1313.

Tobler, W., Deichmann, U., Gottsegen, J., and Maloy, K. (1995), The Global Demography Project, Technical Report 95-6, National Center for Geographic Information and Analysis, University of California, Santa Barbara.

Welch, R. (1980), Monitoring urban population and energy utilization patterns from satellite data. *Remote Sens. Environ.* 9:1–9.